Grand canonical Monte Carlo investigations of electrical double layer in molten salts

Stanisław Lamperski[a] and Jacek Kłos
Department of Physical Chemistry, Faculty of Chemistry, A. Mickiewicz University, Grunwaldzka 6, 60-780 Poznań, Poland

(Received 12 February 2008; accepted 30 April 2008; published online 23 October 2008)

Results of the Monte Carlo simulation of the electrode/molten salt interface are reported. The system investigated was modeled by the restricted primitive model of electrolyte being in contact with the charged hard wall (hard spheres of diameter $d=400$ pm and relative permittivity $\varepsilon_r=10$). The temperature analysis of the mean activity coefficient $\gamma_{\pm}$, heat capacity C_v and radial distribution function, g, indicated the range of temperatures of the study. Calculations for the electrode/electrolyte interface were carried out for temperatures 1300, 1400, and 1500 K and in the range of the electrode charge densities σ from 0.025 to 0.5 C m^{-2}. Singlet distribution functions showed a multilayer structure of the electrolyte in the vicinity of the electrode surface. The structure depended on the electrode charge, but not much on temperature. The capacitance curves had a parabolalike shape with the maximum located at $\sigma=0$. This result is not consistent with the Gouy–Chapman theory, but has been confirmed by the modified Poisson–Boltzmann theory, which includes the correlation and exclusion volume effects. © *2008 American Institute of Physics*.
[DOI: 10.1063/1.2933434]

I. INTRODUCTION

Molten salts as electrolytes have some advantages over aqueous salt solutions, which are traditionally used in electrochemistry, and have broad thermal range of existence in liquid stage and good electrochemical and thermal stabilities. Their application in the electrochemical systems is still being investigated. The pioneering theoretical description of electric double layer capacitance in molten salts was done by Dogonadze and Chizmadjev[1] in the 1960s. The authors expressed the capacitance by the ion-distribution correlation functions. The theory does not describe the potential dependence of capacitance and perhaps that is why Parsons[2] claimed that the theory of electric double layer of molten salts does not exist. Recently, some attempts in the formulation of such a theory had been made by Kisza.[3,4] Kornyshev[5] has derived an analytical expression, based on the theory of the Poisson–Boltzmann lattice-gas model, which describes the double layer capacitance, taking into account the finite ionic volume. His double layer capacitance against electrode potential curve has a bell shape with the maximum at zero potential. Further development of the theory needs, among other things, systematic computer simulations.

There are only several papers devoted to the problem of investigation of the electric double layer in molten salt by molecular simulations. Perhaps, the first credible Monte Carlo (MC) simulations of molten salts were carried out by Larsen and Rodge[6] in the 1970s. The work was devoted to the problem of practical ergodicity of the restricted primitive model applied to the electrolyte solutions and molten salts in MC calculations. The authors found that the practical ergodicity is fulfilled, which, in turn, confirmed the reliability of the MC data in the field mentioned.

Heyes and Clarke,[7] by the use of molecular dynamics (MD), investigated the microscopic boundary between the molten salt and the rigid wall of the electrode. They have found structural ordering close to and in the direction perpendicular to the wall. Distribution functions for tangential planes reveal ion clustering near the electrode surface. The two charged interfaces affect the distribution functions up to the bulk of the systems investigated.

Esnouf *et al.*[8] have investigated the influence of electrode charges and temperature on the ion profiles, diffusion constant, and capacitance by means of the MC method. They observed a positive relation of the inverse capacitance with temperature, which agrees with the results of the mean spherical approximation theory but is contrary to experimental results.[9,10] Higher electrode charges reduce the mobility of ions in the direction perpendicular to the electrode but not in parallel, which is manifested by smaller values of the mean square displacement function. A linear dependence of $\log D$ against $1/T$ implies that diffusion occurs by hopping and that the interface region behaves more like a solid than a liquid.

Lanning and Madden[11] used the MD technique to analyze the interactions of molten KCl confined between rigid charged walls. They have found that the properties of a molten salt near a charged wall are similar to those of the bulk fluid except for the known oscillations in the mean number of ions and charge densities. The molten salt responds very quickly to changes in the surface charge density and also rapidly screens the potential due to the surface charge.

Boda *et al.*[12] have focused on the properties of interfa-

[a]Author to whom correspondence should be addressed. Tel.: +48-61-8291454. FAX: +48-61-829-1505. Electronic mail: slamper@amu.edu.pl.

cial region. They considered ions of the same sizes and investigated the influence of temperature on the double layer capacitance at small electrode charges. Their main result was that below the critical temperature $T_c^*=0.282$ (T^* is the reduced temperature, $T^*=4\pi\varepsilon_0\varepsilon_r dkT/z_-z_+e^2$, ε_0 the vacuum permittivity, ε_r the relative permittivity, d the ion diameter, k the Boltzmann constant, z_i the charge number of species i, and e the elementary charge), the capacitance increases with increasing temperature, while above this temperature the capacitance decreases.

Lamperski[13] carried out simulations of the electrode/electrolyte interface for the equal and unequal ion sizes, of 1:1 and 2:1 salts, at different temperatures (600, 1000, and 1600) but below T_c, and in a wide range of electrode charges. The most important conclusions reported in this work are that the divalent ions increase the integral capacitance of the electric double layer in comparison to that of monovalent ions, the ion size asymmetry leads to strong screening effects, and temperature increases the capacitance at small electrode charges and reduces it at higher charges.

When talking about molten salt interfaces, we should mention the works of Madden and co-workers.[14,15] These authors investigated the liquid/vapor interface of pure molten salts (LiCl and KCl) and their mixtures using the MD method. The ions they studied were of the same and different sizes. They found clearly different density profiles of anions and cations for the different ion sizes (LiCl) while for the same sizes (KCl) the profiles were indistinguishable.

In this paper, we want to repeat the MC simulations of molten salts modeled by charged hard spheres, but this time in the grand canonical MC (GCMC) ensemble. The GCMC technique is recommended for inhomogeneous systems.[16] Also, it allows to some extent the elimination of the practical problem involving ergodicity. The trouble with determination of the bulk electrolyte concentration, which appears in the canonical ensemble simulations, does not exist here, but one must know the activity coefficient corresponding to the concentration desired. We want to find if the salt modeled by the hard sphere and Coulombic interactions can manifest a phase transition at the constant volume of the simulation box. Finally, we want to compare our differential capacitance of the electric double layer with the predictions of the inhomogeneous modified Poisson–Boltzmann (MPB) theory.[17]

II. THE MODEL AND SIMULATION DETAILS

Calculations were performed using the GCMC method. The simulation box was a rectangular prism of the dimensions $W\times W\times L$. Two planar hard walls, impenetrable to ions, represented the electrode surfaces. One of them was charged with a uniform electric surface charge density, σ. The simulation box was replicated in the directions parallel to the electrode surface. We considered the 1:1 electrolyte with ions of the same size. The ions were treated as hard spheres of diameter d with the point electric charge z_ie at the center. The polarizability of the ions was accounted for by the relative electric permittivity ε_r of the continuous medium in which they were immersed. This is the restricted primitive model (RPM) of the electrolyte. The short range interactions between the ions present in the simulation box were calculated explicitly by the minimum image convention. Similarly, the interactions of these ions with the electrode surface and uncharged wall were calculated exactly. The electrostatic interactions of an ion with ions outside the box were estimated with the method introduced by Torrie and Valleau,[18] in which infinitely large charged planes with a square hole for the simulation box are applied. The ion concentration against the electrode surface was described by the singlet distribution function, g. The local ion density number $n(x)$ at a distance x from the electrode surface was related to the bulk density n^0 as follows:

$$g_i(x)=n_i(x)/n_i^0, \quad i=-,+. \tag{1}$$

In the canonical ensemble, the bulk density is calculated by averaging the density profile in the middle part of the simulation box. The required bulk concentration is obtained by small adjustments to the box length, L, or to the number of ions.[19] In the GCMC technique, these exertions are redundant. Now, the bulk electrolyte concentration is the input parameter.

The singlet distribution functions were used to calculate the mean electrostatic potential

$$\psi(x)=-\frac{e}{\varepsilon_r\varepsilon_0}\sum_{i=-,+} z_i n_i^0 \int_{\max(x,d/2)}^{L} g_i(x_1)(x_1-x)\mathrm{d}x_1. \tag{2}$$

The integral capacitance, C_{int}, was calculated from the potential of the electrode, $\psi(0)$,

$$C_{\mathrm{int}}=\sigma/\psi(0). \tag{3}$$

The differential capacitance was not calculated directly because of the lack of precision of our results for this technique. Instead of it, we fitted a third-order polynomial to the $(\psi(0),\sigma)$ points by the least squares method and calculated the derivative numerically although fitting to third-order polynomial may suggest the method developed by Smagala and Fawcett (Ref. 20), our method is different and sufficient for molten salts.

As mentioned above, the GCMC technique was applied to perform the calculations. In the grand canonical ensemble, three quantities are constant: temperature, T, volume, V, and chemical potential, μ. The chemical potential is given at the beginning of the simulation in the form of two factors: concentration c and mean activity coefficient $\gamma_\pm$. Their product gives the mean activity, $a=c\times\gamma_\pm\times 1000$ (to be consistent with the SI units, we introduce the factor 1000 to recalculate from $\mathrm{mol/dm^3}$ to $\mathrm{mol/m^3}$). The simulation consists of three basic moves:

(a) displacement of an ion in the system,
(b) insertion of new ions into the system, and
(c) removal of the ions from the system.

The insertion and removal moves of ions cannot break the electroneutrality of a system. So in the case of 1:1 electrolyte, a pair of ions (one anion and one cation) is exchanged with the system at each move. The displacement of the ion to the new random position is accepted (acc) with the probability given by the Metropolis condition as follows:

$$\text{acc(new config.)} = \min\left\{1, \exp\left[-\frac{u_n - u_o}{kT}\right]\right\}, \tag{4}$$

where u_n and u_o are the potential energies of the new and old configuration of ions, respectively. The next two moves are controlled, according to the following formulas:

(a) insertion

$$\text{acc}(N_+ + N_- \rightarrow N_+ + N_- + 2) = \min\left\{1, \exp\left[-\frac{u(N+2) - u(N)}{kT}\right] + \ln\left(\frac{a_+ V}{N_+ + 1}\right) + \ln\left(\frac{a_- V}{N_- + 1}\right)\right\}, \tag{5}$$

(b) removal

$$\text{acc}(N_+ + N_- \rightarrow N_+ + N_- - 2) = \min\left\{1, \exp\left[-\frac{u(N-2) - u(N)}{kT}\right] + \ln\left(\frac{N_+}{a_+ V}\right) + \ln\left(\frac{N_-}{a_- V}\right)\right\}, \tag{6}$$

where N_+ and N_- are the current numbers of ions, $N=N_- + N_+$, a_+ and a_- the individual ion activities equal here to the mean activity a, $u(N+2)$, $u(N-2)$, and $u(N)$ the energies after insertion, after removal, and before these moves, and V the volume available for ions where

$$V = (L - d)W^2. \tag{7}$$

III. NUMERICAL DETAILS OF THE SIMULATIONS

The simulation box parameters were $W=5063.085$ pm and $L=5800.000$ pm. The difference in the number of ions N_+ and N_- present in the box had to be constant during the simulation to give the desired electrode surface charge σ as follows:

$$\sigma = -e(z_- N_- + z_+ N_+)/W^2. \tag{8}$$

The ion diameter was taken $d=400$ pm as an average of the radii of Cl^-, Br^-, and I^- anions.[21] The density of a system is usually given by the packing fraction η as follows:

$$\eta = \pi d^3 (n_-^0 + n_+^0)/6. \tag{9}$$

In our case, the bulk density numbers of anions and cations are equal ($n_-^0 = n_+^0$) and they depend on the molar concentration of a salt, c,

$$n_i^0 = 1000 c N_A, \tag{10}$$

where N_A is the Avogadro constant. When using the value of the packing fraction, $\eta=0.35$, suggested for molten salts by Larsen,[22] one obtains $c=8.672M$. The bulk relative permittivity of molten salt was taken as $\varepsilon_r=10$ as the average of the common salts.[23] The simulations were carried out for the following electrode charges $\sigma/\text{C m}^{-2}=0.025$, 0.05, 0.1, 0.15, 0.2, 0.25, 0.3, 0.4, and 0.5 ($\sigma^* = \sigma d^2/e = 0.024\,97$, 0.049 93, 0.099 86, 0.149 80, 0.199 73, 0.249 66, 0.299 59, 0.399 46, and 0.599 18, respectively) at three temperatures (see below). The mean activity coefficients $\gamma_\pm$ were obtained from the inverse GCMC simulation (IGCMC) described elsewhere.[24] The number of configurations used to equilibrate the system was 40×10^6. The averages were calculated from the next 100×10^6 configurations. Each simulation was repeated several times to improve the statistics.

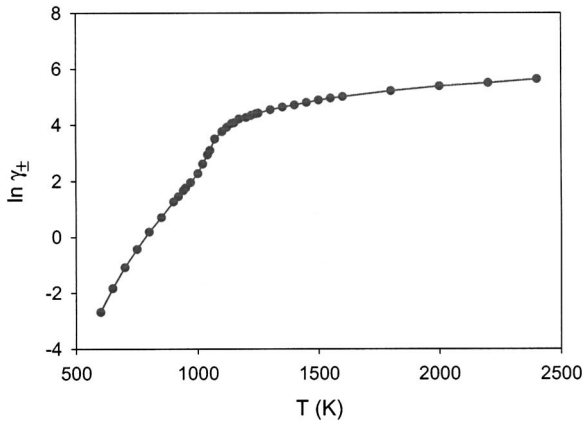

FIG. 1. Temperature dependence of ln $\gamma_\pm$ for a 1:1 equal ion size system at $d=400$ pm, $\varepsilon_r=10$, and $\eta=0.35$ (the IGCMC technique).

Before performing the simulations, we decided to find whether a salt modeled by the hard sphere and Coulombic interactions at constant volume of the simulation box shows any evidence of the presence of a phase transition. According to the traditional Ehrenfest classification at the nth order phase transition, the nth and higher derivatives of the chemical potential against temperature exhibit a discontinuity while the lower derivatives are continuous. The temperature measurements of the heat capacity are another tool to detect the temperature of phase transitions. At the first-order transition, the heat capacity becomes infinite while at the second-order transition it is discontinuous. Currently, the phase transitions are divided into two classes according to the discontinuous or continuous change of the microscopic structure of a substance across the phase transition line.[25]

The important component of the chemical potential is the mean activity coefficient, $\gamma_\pm$. It describes all the deviations from the ideal system behavior. The temperature dependence of ln $\gamma_\pm$ calculated from the IGCMC method[24] is shown in Fig. 1. The monotonic logarithmiclike course of the curve is disturbed in the range of temperatures 900–1200 K where it has a steplike shape. In this range, the curve has two inflection points, but from these results it is hard to predict a discontinuity of the first- or second-order derivate. The temperature dependence of the heat capacity, C_V, calculated from the fluctuation of energy during the MC simulation in the canonical ensemble is shown in Fig. 2. The weak exponential-like decay is disturbed again in the range of temperatures 900–1200 K. This time three peaks are observed in this region, one of them at 1050 K is the highest and well formed. The peaks suggest the presence of structural transformations, which need an additional amount of energy to occur. The presence of the structural transformations confirms the character of the radial distribution functions, g, calculated during the same MC simulations. The distribution functions for like ions at different temperatures are collected

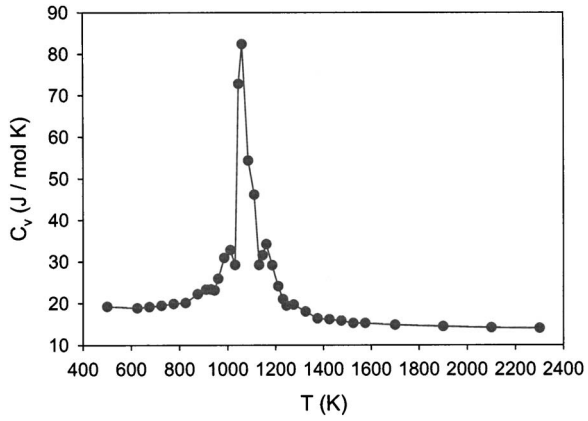

FIG. 2. Temperature dependence of heat capacity, C_V, for a 1:1 equal ion size system at d=400 pm, ε_r=10, and η=0.35 (the canonical ensemble MC technique, $N_-=N_+=128$).

in Fig. 3. A qualitative difference is clearly visible between the curves for 1000 and 1100 K. At higher temperatures, the curves have a sharp maximum at the contact distance. Similar behavior is seen in the like-ion distribution function of the solvent primitive model at high values of the packing fraction.[26] At lower temperatures, the first maximum is shifted towards greater distances, which may suggest the ion pairing effect.[27] However, the configurations we observed at the end of the simulations show, depending on temperature, a more or less regular crystal-like ion structure.

All the evidence presented above does not indicate clearly the type, class (order), and the temperature of the phase transitions because the investigation was performed at a constant volume, not pressure. So, all we can say is that the crystal-like structure occurs in temperatures below 900 K while above 1200 K we have a liquid phase converting into a supercritical fluid with the temperature rise, or a supercritical fluid at once. Many properties of molten salts and their supercritical fluids are similar and some different properties, e.g., pressure, are unimportant for the present studies. That is

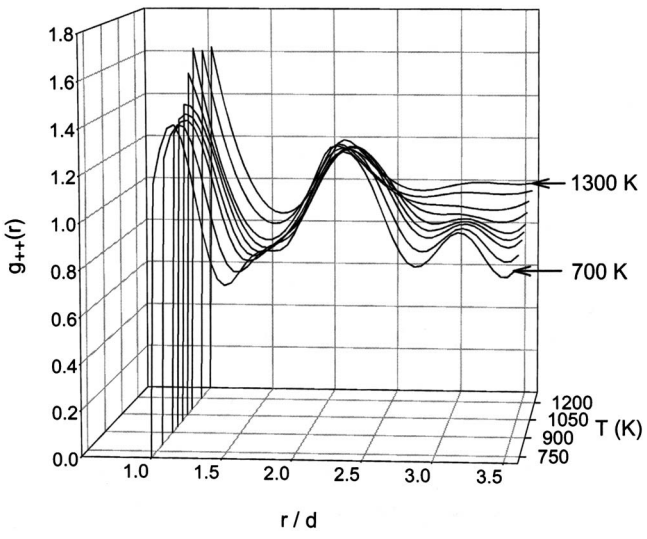

FIG. 3. The like-ion distribution functions $g(r)$ for a 1:1 equal ion size system at T=700, 800, 900, 950, 1000, 1050, 1100, 1200, and 1300 K for d=400 pm, ε_r=10, and η=0.35 (the canonical ensemble MC technique, $N_-=N_+=128$).

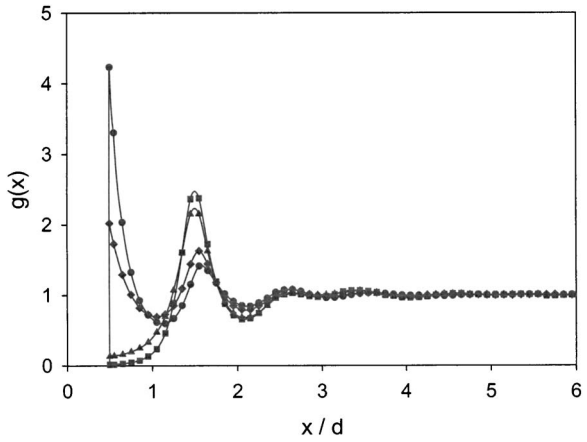

FIG. 4. Singlet distribution functions of cations, $g_+(x)$, for a 1:1 electrolyte at T=1400 K for σ/C m^{-2}=0.025 (circles), 0.15 (diamonds), 0.4 (triangles), and 0.5 (squares) at d=400 pm, ε_r=10, and η=0.35.

why we decided to carry out the investigations above 1200 K, namely, at T=1300, 1400, and 1500 K (T^*=0.3112, 0.3352 and 0.3591, respectively). It means that we were above the critical temperature, T_c^*=0.282 (1179 K), reported by Boda *et al.*[12] The mean activity coefficients $\gamma_\pm$ corresponding to the temperatures at which the simulations were carried out were 99.407 93, 117.689 04, and 137.589 79, respectively.

IV. RESULTS AND DISCUSSIONS: THE PROPERTIES OF THE ELECTRIC DOUBLE LAYER

The singlet distribution function of ions, also called the relative ion density, is the first average obtained from the simulation. Figures 4 and 5 show the singlet distribution functions of cations and anions, respectively, calculated for the electrode charges σ/C m^{-2}=0.025, 0.15, 0.4, 0.5 (σ^*=0.024 97, 0.149 80, 0.399 46, and 0.599 18, respectively). The results are weakly dependent on temperature, so we present them here for T=1400 K. A similar lack of temperature effect was reported by Boda *et al.*[12] The curves exhibit several maxima progressively damping with the distance from the electrode. This behavior is characteristic of

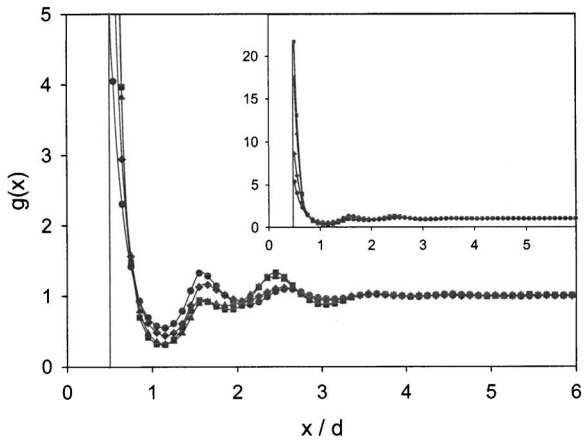

FIG. 5. Singlet distribution functions of anions, $g_-(x)$, for a 1:1 electrolyte at T=1400 K for σ/C m^{-2}=0.025 (circles), 0.15 (diamonds), 0.4 (triangles), and 0.5 (squares) at d=400 pm, ε_r=10, and η=0.35.

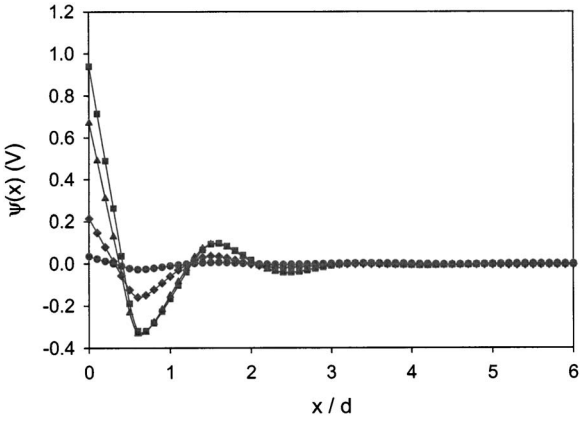

FIG. 6. The profile of mean electrostatic potential, $\psi(x)$, for a 1:1 electrolyte at $T=1400$ K and for $\sigma/\mathrm{C\,m^{-2}}=0.025$ (circles), 0.15 (diamonds), 0.4 (triangles), and 0.5 (squares) at $d=400$ pm, $\varepsilon_r=10$, and $\eta=0.35$.

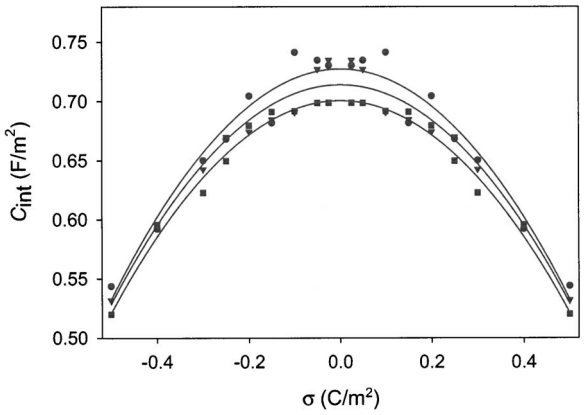

FIG. 7. The integral capacitance of the electrical double layer, C_{int}, as a function of the surface charge density σ for a 1:1 electrolyte at $T/K=1300$ (circles), 1400 (triangles), and 1500 (squares); curves—the least squares fitting results ($d=400$ pm, $\varepsilon_r=10$, and $\eta=0.35$).

high density systems and indicates a multilayer structure in the interfacial region. The influence of the electrode charge on the distribution of ions is significant. At the positive electrode charges, there is a general tendency to remove the cations from the vicinity of the electrode surface. At the contact distance, the cation distribution function falls from about 4.23 at $\sigma=0.025$ C m^{-2} to almost 0 at $\sigma=0.5$ C m^{-2}. This is a result of a competition between the steric effect and electrostatic repulsion. Simultaneously, the second maximum at $x/d\approx 1.5$ rises from about 1.4 to 2.5 and is slightly shifted towards the electrode surface. Similar unexpected behavior was observed earlier for aqueous divalent electrolytes.[28,29] Different behavior was observed for anions. Their amount in the vicinity of the positively charged electrode surface increases with increasing surface charge. The first maximum (at a contact distance) is rising from about 5.4 at $\sigma=0.025$ C m^{-2} to almost 22 at $\sigma=0.5$ C m^{-2}, but the height of the second maximum falls, while that of the third one rises with increasing electrode charge. Again, a similar behavior was noted for divalent anions in aqueous solution[28,29] with one exception that the third maximum was weakly pronounced.

The profile of the mean electrostatic potential, ψ, at $\sigma/\ \mathrm{C\,m^{-2}}=0.025$, 0.15, 0.4, 0.5, and $T=1400$ K is shown in Fig. 6. The curve exhibits damped oscillations, which vanish at a distance of four diameters from the electrode surface. In the vicinity of the electrode surface, the electrostatic potential falls rapidly and the curve has a negative minimum value at $x/d\approx 0.65$. The second distinct minimum is at $x/d\approx 2.45$. The temperature effect is small. Aqueous divalent electrolytes exhibit only one minimum with the depth depending on the electrode charge. Subsequent oscillations are smaller.

The integral capacitance, C_{int}, results are presented in Fig. 7. Although they are scattered (mainly at small electrode charges and at lower temperature), the fit of the second-order polynomial reveals a very probable dependence of the integral capacitance on the electrode charge and on the temperature. The C_{int}-σ curves have a parabolalike shape with the maximum located at $\sigma=0$. However, because of large scatter at 1300 K, we cannot exclude in the neighborhood of $\sigma=0$, a shallow capacitance minimum with a maximum on either side. The results shown in Fig. 7 are opposite to the Gouy–Chapman[30,31] predictions. The capacitance decreases with increasing temperature in the whole investigated range of σ. This effect is in agreement with the general conclusions following from the Gouy–Chapman theory and corresponds well with the predictions of Boda *et al.*[12] above their critical temperature.

We calculated the differential capacitance, C_{diff}, which is the experimentally available quantity, as described earlier. The results for 1400 K are shown in Fig. 8. The curve is steeper, now. As the capacitance maximum located at $\sigma=0$ seems to be a surprising result, we decided to collate it with the predictions of recent theories. The MPB theory developed by Outhwaite and Bhuiyan[17] is one of the efficient theories of the electric double layer.[32] The version with the new exclusion volume term[33] is more adequate for systems with strong electrostatic interactions.[32] When using MPB, we meet the numerical problem: The equations can be solved for a limited range of electrode charges ($|\sigma|\leqslant 0.22$ C m^{-2}) and not too high packing fraction ($\eta\leqslant 0.27$). Although the value of $\eta=0.35$ used in our MC calculations was slightly greater, we present in Fig. 8 also the MPB (Ref. 33) predictions at

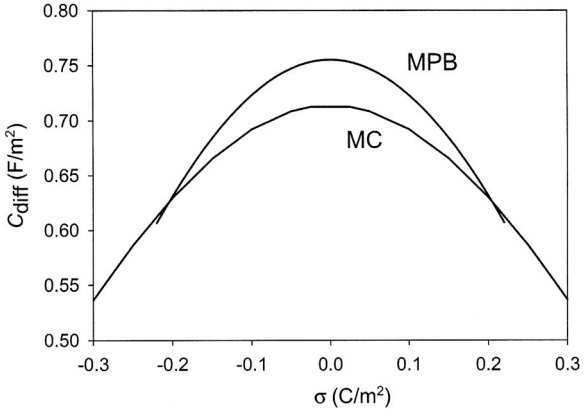

FIG. 8. The MC and MPB differential capacitance of the electrical double layer, C_{diff}, as a function of the surface charge density σ for a 1:1 electrolyte at $T=1400$ K, $\eta=0.35$ (MC) and 0.27 (MPB), $d=400$ pm, and $\varepsilon_r=10$.

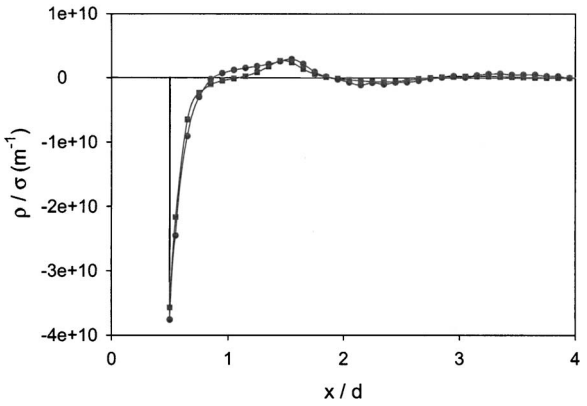

FIG. 9. The local charge density, $\rho(x)$, of the electrolyte related to the electrode surface charge density σ at $\sigma/\mathrm{C\,m^{-2}}=0.015$ (circles) and 0.5 (squares), $T=1400$ K, $d=400$ pm, $\varepsilon_r=10$, and $\eta=0.35$.

$\eta=0.27$. The qualitative agreement is surprisingly good. The curve has a parabolalike shape with the maximum at $\sigma=0$.

The presented charge dependence of the capacitance needs some comments. In aqueous 1:1 RPM electrolytes, the capacitance decreases, but only at very high electrode charges.[34,35] This effect is explained by the formation of the second layer of counterions.[19] Formation of this layer is due to the packing effect and electrostatic repulsion between counterions in the first layer, which becomes overcrowded. The explanation of the capacitance behavior of molten salts cannot be simply concluded from the singlet distribution functions. Therefore, we calculated the quotient of the volume charge density, $\rho(x)$, of ions by the electrode charge density, σ. The dependence of this quantity on the distance from the electrode surface at $\sigma/\ \mathrm{C\,m^{-2}}=0.025$ and 0.5 is shown in Fig. 9. The curves are nearly identical, but in the range $0.5<x/d<0.75$ and $0.75<x/d<1.5$ there are visible spans between the curves. When the electrode charge increases, some amount of negative charge is transferred from the first region to the second one, neutralizing the positive charge occurring in this latter region. We can expect that the mechanism of charge transfer is similar to that of the aqueous RPM electrolytes described above. Thus, the explanation of the capacitance behavior is similar to that of aqueous electrolytes with the difference that instead of second counterion layer formation we observe neutralization of the coion charge by counterions. There is another aspect of this effect. Even at uncharged electrode surface, the first layer is full of anions and cations because of high density of a system. At the charged electrode, the counterions do not have easy access to the first layer as this layer is full of ions and the strong interion interactions stabilize their structure. In this case, the counterions accumulate at the second layer. Thus, the capacitance decrease is explained again by the increase in the thickness of the electric double layer. However, contrary to the aqueous RPM electrolytes, this effect occurs even at small electrode charges.

Comparison of our simulation results with experimental ones is not easy. The early experimental results on the differential capacitance of the electric double layer in molten salts done mainly by the Soviet scientists[36] in the early 1960s show a parabola shape with a deep minimum or in some cases with two minima. However, recently, these results have been criticized by Kisza[4] as the faradic current was ignored. Kisza *et al.*[37] claimed that the differential capacitance of the electric double layer in molten salts has a completely different shape: There is a flat shallow minimum surrounded by two small maxima. At strong cathodic and anodic polarizations, the capacitance decreases. Presumably, the extension of the present model by considering the ion size asymmetry, soft sphere interactions, image forces, hyperpolarizability, etc., will give more realistic results.

V. SUMMARY

The GCMC results are reported for the electric double layer formed by a symmetrical molten salt at different electrode charges and temperatures. The main achievement of the investigation is the determination of the double layer differential capacitance dependence on the electrode surface charge density. The capacitance curves have a parabolalike shape with the maximum located at $\sigma=0$. Although this result is contrary to the predictions of the Gouy–Chapman theory,[30,31] it is confirmed by the more recent MPB theory,[33] which includes the correlation and exclusion volume effects. The predictions of the Poisson-Boltzmann theory extended by the exclusion volume term also support this result.[38–40] Here, the agreement is qualitative only, but indicates that the hard core interactions play an important role in the inversion of the classical Gouy–Chapman parabola. Recently, Kornyshev[5] has shown that at high densities typical of molten salts or ionic liquids the capacitance curve of the electric double layer has the inverted parabola shape.

The second problem we have pointed out in this paper is the phase transition of salts modeled by the hard sphere and Coulombic interactions at a constant volume of the simulation box. The temperature analysis of the mean activity coefficient, the heat capacity, and the ion radial distribution functions suggested melting of the crystal-like phase somewhat below 1200 K. This temperature corresponds well with the critical temperature $T_c^*=0.282$ (1179 K) determined by Boda *et al.*[12] They reported that below $T^*=0.141$ (590 K), the ions tended to form chainlike structures along the z-axis of the simulation cell. We also observed these chains below 600 K. However, contrary to Boda *et al.*,[12] we found some remains of the chains even at higher temperatures, but below 1200 K.

ACKNOWLEDGMENTS

The authors are very grateful to Professor C. W. Outhwaite and Professor E. Dutkiewicz for their comments and suggestions and to Professor C. W. Outhwaite and Professor L. B. Bhuiyan for making their MPB program available. Financial support from Adam Mickiewicz University, Faculty of Chemistry, is appreciated.

[1] R. R. Dogonadze and Yu. Chizmadzhev, Dokl. Akad. Nauk SSSR **157**, 994 (1964).
[2] R. Parsons, Chem. Rev. (Washington, D.C.) **90**, 813 (1990).
[3] A. Kisza, J. Electroanal. Chem. **534**, 99 (2002).
[4] A. Kisza, Electrochim. Acta **51**, 2315 (2006).
[5] A. A. Kornyshev, J. Phys. Chem. B **111**, 5545 (2007).

[6] B. Larsen and S. A. Rogde, J. Chem. Phys. **68**, 1309 (1978).
[7] D. M. Heyes and J. H. R. Clarke, J. Chem. Soc., Faraday Trans. 2 **77**, 1089 (1980).
[8] R. M. Esnouf, A. C. D. Smith, and P. J. Grout, Philos. Mag. A **58**, 27 (1988).
[9] A. D. Graves, J. Electroanal. Chem. Interfacial Electrochem. **25**, 349 (1970).
[10] A. D. Graves, J. Electroanal. Chem. Interfacial Electrochem. **25**, 357 (1970).
[11] O. J. Lanning and P. A. Madden, J. Phys. Chem. B **108**, 11069 (2004).
[12] D. Boda, D. Henderson, and K.-Y. Chan, J. Chem. Phys. **110**, 5346 (1999).
[13] S. Lamperski, Molten Salts Conference Proceedings, Euchem, 2004 (unpublished), pp 218–224.
[14] A. Aguado, W. Scott, and P. A. Madden, J. Chem. Phys. **115**, 8612 (2001).
[15] A. Aguado and P. A. Madden, J. Chem. Phys. **117**, 7659 (2002).
[16] D. Frankel and B. Smit, *Understanding Molecular Simulation: From Algorithms to Applications* (Academic, San Diego, CA, 1996), p. 114.
[17] C. W. Outhwaite and L. B. Bhuiyan, J. Chem. Soc., Faraday Trans. 2 **79**, 707 (1983).
[18] G. M. Torrie and J. P. Valleau, J. Chem. Phys. **73**, 5807 (1980).
[19] S. Lamperski and L. B. Bhuiyan, J. Electroanal. Chem. **540**, 79 (2003).
[20] T. G. Smagala and W. R. Fawcett, J. Phys. Chem. B **1443**, 111 (2007).
[21] R. D. Shanon and C. T. Prewitt, Acta Crystallogr., Sect. B: Struct. Crystallogr. Cryst. Chem. **25**, 925 (1969).
[22] B. Larsen, J. Chem. Phys. **65**, 3431 (1976).
[23] *CRC Handbook of Chemistry and Physics*, 86th ed., edited by D. R. Lide (CRC, Boca Raton, FL, 2005), pp. 12–44.
[24] S. Lamperski, Mol. Simul. **33**, 1193 (2007).
[25] C. Garrod, *Statistical Mechanics and Thermodynamics* (Oxford University Press, New York, 1995), p. 155.
[26] J. Reščič, V. Vlachy, L. B. Bhuiyan, and C. W. Outhwaite, J. Chem. Phys. **107**, 3611 (1997).
[27] J. M. Caillol, D. Levesque, and J. J. Weis, Mol. Phys. **69**, 199 (1990).
[28] G. M. Torrie and J. P. Valleau, J. Phys. Chem. **86**, 3251 (1982).
[29] S. L. Carnie and G. M. Torrie, Adv. Chem. Phys. **56**, 141 (1984).
[30] G. Gouy, J. Phys. (Paris) **9**, 457 (1910).
[31] D. L. Chapman, Philos. Mag. **25**, 475 (1913).
[32] L. B. Bhuiyan and C. W. Outhwaite, Phys. Chem. Chem. Phys. **6**, 3467 (2004).
[33] C. W. Outhwaite and S. Lamperski, Condens. Matter Phys. **4**, 739 (2001).
[34] Z. Tang, L. E. Scriven, and H. T. Davis, J. Chem. Phys. **97**, 494 (1992).
[35] S. Lamperski and A. Zydor, Electrochim. Acta **52**, 2429 (2007).
[36] See, for example, N. A. Ukshe, N. G. Bukun, and D. I. Lejkis, Zh. Fiz. Khim. **36**, 2322 (1962).
[37] A. Kisza, J. Kaźmierczak, and B. Meisner, Pol. J. Chem. **78**, 561 (2004).
[38] S. Lamperski (unpublished).
[39] M. S. Kilic, M. Z. Bazant, and A. Ajdari, Phys. Rev. E **75**, 021502 (2007).
[40] K. B. Oldham, J. Electroanal. Chem. **613**, 131 (2008).